American Mineralogist, Volume 89, pages 1525–1532, 2004

Mass balance during retrogression of eclogite-facies minerals in the Rongcheng eclogite, eastern Sulu ultrahigh-pressure terrane, China

TIAN N. YANG,[1,*] ZHI Q. XU,[1] AND MARY LEECH[2]

[1]Institute of Geology, Chinese Academy of Geological Sciences, Beijing, 100037, China
[2]Geological and Environmental Sciences, Stanford University, Stanford, California 94305, U.S.A.

ABSTRACT

Eclogite from Rongcheng in the easternmost part of the Sulu ultrahigh-pressure metamorphic terrane has broken down (at least partially) with the formation of coronae of spinel + anorthite around kyanite, symplectites of pargasite + plagioclase around garnet, and symplectites of diopside + plagioclase after omphacite. Textural evidence and microprobe analysis indicate that this breakdown was generated by discontinuous reactions. Quantification of material transfer and textural information suggest that the reaction mechanism involved local exchange of components among the three major minerals (omphacite, garnet, and kyanite) during dissolution and discontinuous precipitation, coupled with exchange between eclogites and their host rocks. The symplectite formed after omphacite gained Al and minor Si and Na from its surroundings, and lost Mg, Ca, and minor Fe to its surroundings. Formation of the symplectite around garnet was accompanied by gain of Ca, Al, Si, Na, and H_2O, and by loss of Mg and Fe^{2+} to its surroundings. Coronae around kyanite gained Ca, Fe, Mg, and minor Si, and provided Al to their surroundings. Material exchange between eclogite and host rocks occurred as well: eclogite gained minor Al, Na, and H_2O from the host rocks, and provided Mg, Fe, and Ca to the host rocks. Pressure and temperature estimation using THERMOCALC yielded a lower temperature (655 ± 70 °C) and higher pressure (1.3 ± 0.2 GPa), which values contrast with estimates made by other authors. Strong deformation may have created a path for ingress of hydrous fluids, then resulted in a localized lower T and/or higher *P*.

INTRODUCTION

Corona and symplectite textures in high-grade metamorphic rocks are mineral reactions "written in stone" (Sederholm 1916, cited in Johnson and Carlson 1990). They provide us with an opportunity to understand the reactions occurring within the rocks as a result of changing pressure and temperature, as well as the mechanism of such reactions (Carlson and Johnson 1991; Markl et al. 1998). These non-equilibrium textures are common in high-pressure (HP) or ultrahigh-pressure (UHP) eclogites, and reveal information about the eclogitization of gabbros or granulites (Mørk 1985; Rubie 1990; Zhang and Liou 1997; Austrheim 1998), as well as the retrograde metamorphism corresponding to the exhumation of the HP or UHP metamorphic rocks (Wikström 1970; Mysen and Griffin 1973; Liati and Seidel 1996; Godard and Mabit 1998; Möller 1998).

The Sulu ultrahigh-pressure metamorphic (UHPM) terrane, defined mainly by the occurrence of numerous coesite-bearing eclogite lenses, is located in the eastern part of the Qinling-Tongbai-Dabie-Sulu orogenic belt (Fig. 1), which is the suture zone formed from the collision between the Sino-Korean craton to the north and the Yangtze craton to the south (Xu et al. 1992; Wang and Liou 1991; Cong and Wang 1994). Coesite inclusions in zircon from country rocks indicates that a substantial crustal component in the Sulu UHPM terrane was subducted to mantle depths and later returned to the surface (Ye et al. 2000a; Liu et al. 2001). Studies of metamorphic *P-T* conditions and *P-T-t* paths (Yang et al. 1993, 1998; Wang et al. 1993, 1996; Zhang et al. 1995; Wallis et al. 1997; Wang et al. 1995) suggest that the peak UHP temperature increased from west to east, implying that the eastern part of the Sulu terrane experienced the highest peak metamorphic temperature. Regional tectonic analysis and radiometric dating of the collisional orogen have yielded similar results (Yin and Nie 1993). Recently, exsolution lamellae of clinopyroxene identified within garnet grains (Ye et al. 2000b), and other evidence from garnet peridotites (Yang et al. 1993), indicate that the eastern part of the Sulu UHPM terrane experienced peak pressures over 6 GPa, suggesting that this area also may have had the highest peak metamorphic pressure.

In the Rongcheng area, the easternmost part of the Sulu UHPM terrane (see Fig. 1), eclogites have commonly been overprinted by a retrograde granulite-facies metamorphism (700–800 °C, 0.7–1.2 GPa) due to isothermal decompression, which resulted in the formation of spectacular coronae and symplectite textures (Wang et al. 1993; Nakamura and Hirajima 2000). In some retrograde eclogites, coesite inclusions within garnet porphyroblasts have been identified (Wang et al. 1993). These non-equilibrium textures preserve information about mineral reactions and are worthy of detailed study, as they could reveal the evolutionary history of the eclogite during its exhumation. Furthermore, incompletely transformed rocks provide a laboratory for the study of reaction kinetics (Austrheim 1998).

In a closed system, most metamorphic coronae are reaction rims between two reactant minerals (Ashworth and Chambers

* E-mail: yangtn@cags.net.cn

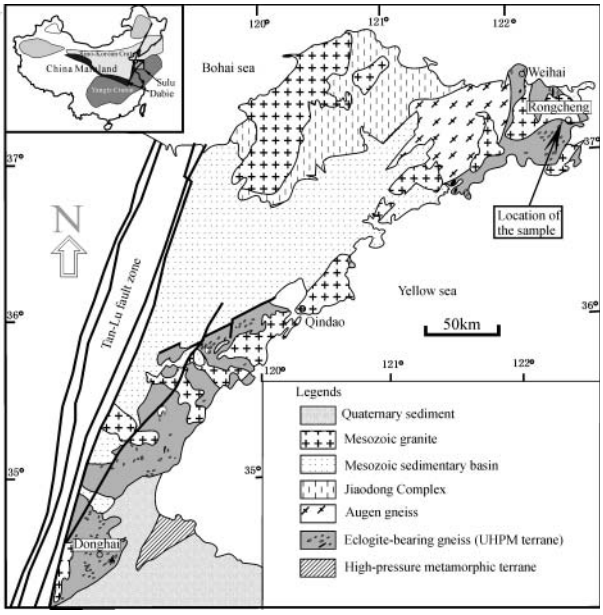

FIGURE 1. Geological map of the Sulu region showing major tectonic units, distribution of eclogites, and the location of the studied Rongcheng eclogite.

2000, and references therein). In many cases, the growth of a corona is related chemically to the reaction that occurs within an adjacent or nearby domain (Rubie 1990). Symplectites are mineral intergrowths produced by solid-state reactions (Johnson and Carlson 1990); perpendicular to the reaction front, elongate grains grow from a single reactant mineral (Ashworth and Chambers 2000). Symplectites of Di + Pl (minerals abbreviations after Kretz 1983) after omphacite in an HP or UHP rock have been studied extensively (Mysen and Griffin 1973, and references therein; Liati and Seidel 1996; Möller 1998; Godard and Mabit 1998). Four models have been proposed to explain the formation of the symplectite: (1) Eskola (1921, cited in Mysen and Griffin 1973) suggested that symplectite was the result of exsolution of the plagioclase components from a jadeitic pyroxene; (2) Mysen and Griffin (1973) and Wikström (1970) concluded that the oxidation of Fe in the parent omphacite could lead to formation of a symplectite of Di + Pl without gaining extra silica; (3) Holland (1980 and references therein) and Anovitz (1991), among others, interpreted the symplectites as the result of the solid-solid reaction of the Jd, Ca-Ts, and the Eskola component in omphacite with extra SiO_2, with the Di component being a residue, forming a symplectite with the produced Pl, provided that silica is available; and (4) Godard and Mabit (1998) proposed that the solid-solid reaction between omphacite and kyanite in a closed system could result in a symplectite. However, no one has documented the mass balance among the three major minerals in a retrograde eclogite in detail.

In the retrograde kyanite-bearing eclogite investigated in this study, coronae or symplectites have replaced all of the three major minerals (omphacite, garnet, and kyanite). Omphacite, including some inclusions in garnet but not in kyanite, is replaced by a symplectite of Di + Pl. Kyanite, except some inclusions in garnet, is partially replaced by a symplectic intergrowth of Pl+Spl (coronae). No sapphirine or corundum has been identified in the Rongcheng eclogite although they are commonly found in other granulite-facies-retrograde eclogites in this area (Nakamura and Hirajima 2000). Garnets are commonly surrounded by intergrowths of Pl + Prg (symplectite). These micro-textures make it possible to estimate quantitatively the material transfer relating to the breakdown of the three minerals based on the method developed by Gresens (1967).

In this paper, retrograde textures are described in detail, and the material transfer responsible for their formation is calculated. In addition, these data are used to discuss mineral reactions, the material exchange among the three major eclogite phases, and mass transfer between the eclogite and its host rocks.

OCCURRENCE AND PETROLOGY

The retrograde-eclogite bodies are located 4 km west of Rongcheng City, in the easternmost part of the Sulu UHPM terrene (122°6′36″E, 37°9′49″N, see Fig. 1). Six discrete eclogite layers (20 to 500 cm thick), found within garnet-bearing gneiss, are exposed in 50 × 50 m quarry; these six layers display no macroscopic banding, mineral segregation, or other compositional heterogeneity.

The retrograde eclogites are dark green in hand sample and consist of large (0.5–5 mm) garnet and kyanite porphyroblasts, and matrix minerals of lath-like omphacite pseudomorphs and plagioclase laths (Fig. 2a). Rutile grains are scattered throughout the rock and are replaced partially by titanite; minor quartz grains occur in the matrix. Based on point counting (32,400 points over four thin-sections) and molar volume data of Holland and Powell (1998), the restored modal mineral composition (mol%) of the eclogite is: omphacite (symplectite after omphacite) = 77; kyanite + coronae (primary kyanite) = 11; garnet + symplectite (primary garnet) = 8; and accessory minerals (quartz, rutile, and opaque minerals) = 3–4. Taking into account the volume expansion (see Table 1; F_v, estimated by mass-balance using Eq. 2) due to the decompression retrogression, the modal mineral composition (mol%) is: omphacite = 70; garnet = 11–12; kyanite = 12–13; and accessory minerals = 5–6.

The garnet porphyroblasts are elongated, with their long axes parallel to the omphacite pseudomorphs (Fig. 2a). Around these porphyroblasts, inhomogeneous symplectite intergrowths of radial vermicular pargasite and plagioclase occur (Figs. 2b, 2c, 2d). The symplectite textures are generally developed much better at the ends of elongate porphyroblasts (Fig. 2c). Rare granular edenite grains adjacent to garnet grains may indicate grain shape re-adjustment (Fig. 2b).

Quartz inclusions are common within the garnet grains (Fig. 2e); radial fractures around quartz inclusions in garnet suggest they formed as a result of the volume increase accompanying the coesite to quartz transformation. Several inclusions of omphacite pseudomorph and kyanite also occur within the garnet (Figs. 2d, 2e, and 3c). Radial fractures around the inclusions in the garnet indicate a volume increase when the pseudomorphs were formed.

Kyanite grains are partly to completely replaced by coronae that have two parts (Figs. 2a, 2b, 3a, and 3b): the inner part is composed of an intergrowth of radial vermicular spinel set in a plagioclase matrix, and the outer part consists solely of plagioclase (Figs. 2a, b, 3a, and 3b). The radial vermicular spinel

TABLE 1. Material transfer calculation for the omphacite, garnet, kyanite, rutile, and whole-rock systems in the Rongcheng retrograde eclogite

	Whole rock*	Rt Sys.	Omp Sys.	Grt-Sys.	Ky-Sys.		
Mol%†		3 (50%)	70 (100%)	12 (10%)	13 (80%)		
	(1)	(2)	(3)	(4)	(5)	(6)	(7) = (5) – (6)
					Whole corona	Inner corona	Outer corona
Si	+0.0293	0.034	+0.027	+0.3355	+0.0564	–0.395	+0.4514
Al	+0.1056	0.004	+0.226	+0.3366	–0.5442	–0.9788	+0.4346
Mg	–0.1821	0	–0.263	–0.6970	+0.0955	+0.0955	0
Ca	–0.0420	0.034	–0.141	+0.4926	+0.4882	+0.2754	+0.2128
Fe^{2+}	+0.0016	0	–0.002	–0.8605	+0.1279	+0.1281	–0.0002
Na	+0.0087	0	+0.003	+0.2737	+0.0315	+0.0192	+0.0123
Fe^{3+}	–0.001	0	–	–0.0794	–	–	–
OH	+0.0031	+0.06	–	+0.1802	–	–	–
F_v		2.9	1.39	1.29	1.03	1.3	0.82

* (1) = (2) × 0.03 × 0.5 + (3) x 0.7 × 1 + (4) × 0.12 × 0.1 + (5) × 0.13 × 0.

† Mol% shows modal mineral composition of the Rongcheng eclogite in this study, the volume expansion due to retrogression has been taken into account. Percentages in parentheses are the decomposition ratio of the mineral, which is used to calculate mass transfer of the whole-rock system. For F_v, see Equation 2 in the text.

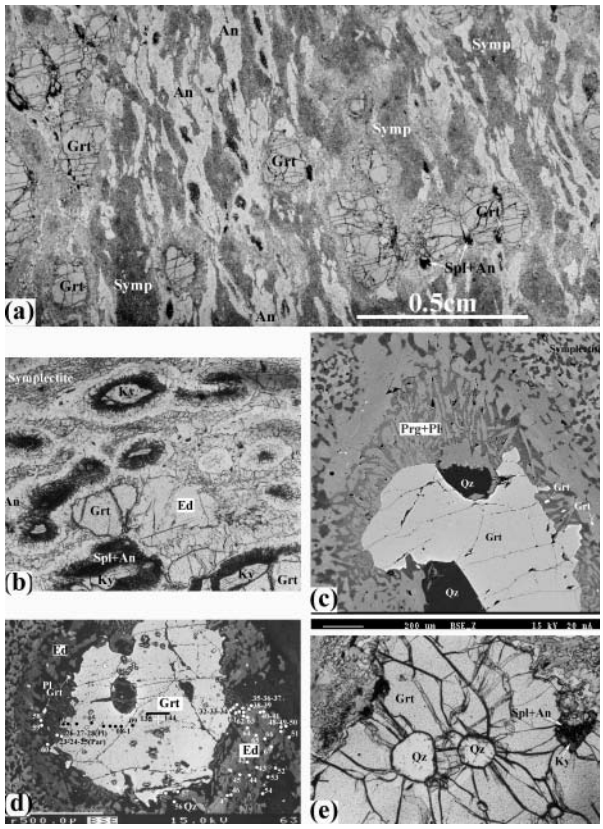

FIGURE 2. Photomicrographs showing microtextures found in the Rongcheng retrograde eclogite: **(a)** remnant garnet porphyroblasts are enclosed within a symplectite (Symp) matrix. The symplectites after omphacite and kyanite are lath-like; **(b)** Spl + An coronae around kyanite occur only where kyanite is in contact with omphacite pseudomorphs; **(c)** symplectite of Prg + Pl is well-developed adjacent to a garnet porphyroblast; **(d)** a garnet porphyroblast surrounded by variably developed Prg + Pl symplectite; and **(e)** quartz inclusions with radial fractures in a garnet porphyroblast. Numbered points show the locations of microprobe analysis sites portrayed in Figures 4 and 5.

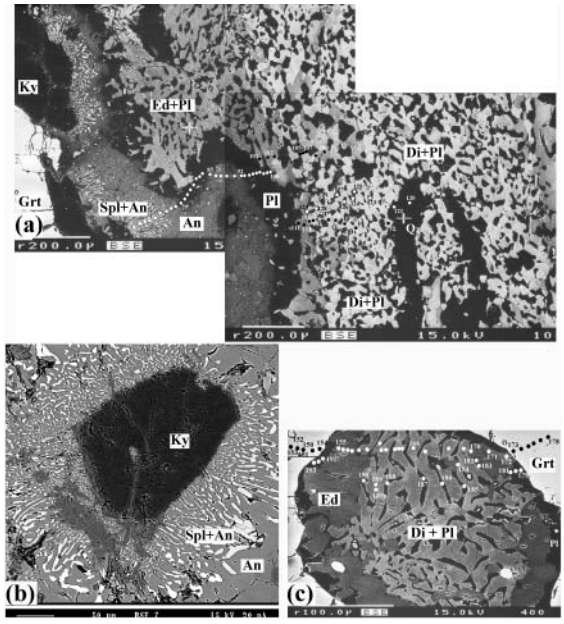

FIGURE 3. Back-scattered electron images show mineral assemblages: **(a)** around a kyanite grain, the coronae occur only where kyanite is in contact with symplectite. Where kyanite is in contact with garnet, no coronae form. Between the coronae and the symplectite there is a film (reaction rim) of plagioclase (Pl). Edenite occurs within the symplectite (Ed + Pl); **(b)** kyanite surrounded by the corona that its inner part consists of Spl + An and its outer part solely anorthite; **(c)** inclusion symplectite within a garnet porphyroblast; in its rim, diopside is replaced by edenite. Abbreviations are the same as in Figure 2.

in the inner part grew perpendicular to the corona boundary. Furthermore, the coronae surrounding kyanite occur only where kyanite is in contact with omphacite; no coronae occur at the contacts with garnet, indicating the coronae result from a kyanite-omphacite reaction. Quartz and omphacite inclusions are common in kyanite porphyroblasts, no reaction occurs between the inclusions and their host mineral.

Omphacite, including inclusions within garnet but not within kyanite, has broken down to symplectite (Figs. 2a, 3a, and 3c). The matrix symplectite consists of an intergrowth of vermicular diopside and plagioclase. The diopside is altered unevenly to edenite, mainly along the rim of the symplectite. Symplectite is surrounded by a film of plagioclase (An_{35}) (Fig. 3a). The presence of edenite does not correlate with any difference in An content of the plagioclase, indicating that edenite and diopside are coeval. Distributed among the matrix symplectites are lath-

like plagioclase grains in which kyanite + coronae are enclosed locally (Fig. 2a).

Therefore, from a kyanite core to its adjacent symplectite after omphacite, the following mineral phases occur successively (Fig. 3a):

Ky → vermicular Spl + Pl (An_{90}) [inner corona] → Pl (An_{90}) [outer corona] → Pl (An_{35}) [film around symplectite] → Ed + Pl (An_{30}) [altered symplectite] → Di + Pl (An_{30}) [symplectite]

From a garnet porphyroblast to the adjacent symplectite after omphacite, the succession of mineral phases is as follows (Fig. 2c):

Grt → Prg + Pl (An_{80}) [symplectite after Grt] → Ed + Pl (An_{30-45}) [altered symplectite] → Di + Pl (An_{30}) [symplectite replacing Omp]

The inclusion symplectite retains the shape of the original omphacite; its core consists of an intimate vermicular intergrowth of plagioclase and diopside, and its rim consists of anhedral plagioclase and edenite (Fig. 3c). This texture suggests that mineral shape and composition readjustment occurred locally.

MINERAL CHEMISTRY

The mineral compositions (Table 1) were obtained by a wavelength-dispersive spectroscopy electron microprobe (CAMECA SX100) at the Institute of Mineralogy, Heidelberg University, Germany. CAMECA-supplied natural mineral and synthetic oxide standards were used for the major elements. The counting time was 20 seconds with a sample current of 10 nA and an acceleration voltage of 15 kV. The mineral formulae were calculated by MINPET software, version 2.0. Ferric iron was calculated assuming stoichiometry after Droop (1987).

Garnet

Detailed analyses of several garnet grains show two types of compositional zoning: (1) garnet porphyroblasts with rims partially replaced by Prg + Pl symplectite have slight compositional zoning in which Mg decreases and Ca increases from core to rim (Figs. 4a and 4b); and (2) around the inclusion symplectite (Fig. 3c), chemical zoning is more extensive, being characterized by a significant increase in Fe^{2+} and a corresponding decrease in Mg from core to rim whereas Ca increases slightly from core to rim (Figs. 4c and 4d).

Type (1) garnet zoning is not very common in eclogite, suggesting that the chemical potential of Ca in the garnet is low relative to the matrix, which drives the Ca-Mg exchange between the garnet and the matrix during or after the formation of the Prg + Pl symplectite. This suggestion is consistent with our mass-transfer estimate (see Table 1). Type (2) garnet zoning is common, and generally has been interpreted as resulting from Fe-Mg exchange between the garnet and the original omphacite during cooling from the peak metamorphic temperature down to temperatures where diffusion rates were no longer high enough to homogenize the garnet (Ghent 1988). These two types of garnet likely formed at different stages. The type (2) garnet formed earlier and was destroyed when Prg + Pl symplectite replaced garnet starting from the rims.

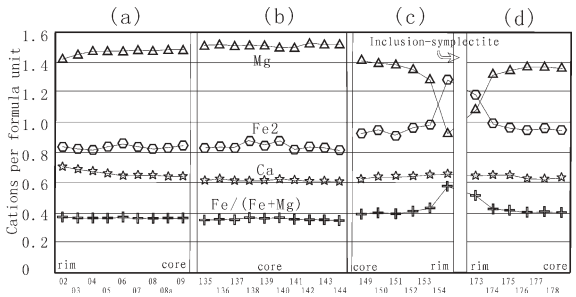

FIGURE 4. Compositional profiles of garnet porphyroclasts: **(a)** from rim to core in Figure 2d; **(b)** in the core of the garnet shown in Figure 2d; and **c** and **d** across inclusion symplectite in Figure 3c. Numbers along the bottom of the figure are microprobe analysis points shown in Figures 2 and 3.

Pyroxenes

Diopside occurs mainly in symplectite after omphacite (see Fig. 3a), but is also found in the inclusion symplectite. The diopside is unzoned; average compositions are listed in Table 1. The Jd component of diopside is slightly higher in the inclusion symplectite but the Wo + En + Fs components are lower than matrix diopside (see Table 2). The absence of zoning in the symplectite suggests that the reaction rate was high and local equilibrium was attained. Omphacite only occurs as inclusions in kyanite porphyroblasts and contains 32 mol% Jd (see Table 2); this omphacite composition is used to estimate material transfer during its decomposition.

Plagioclase

Plagioclase occurs in several ways: (1) in both matrix and inclusion symplectite as Di + Pl after omphacite; (2) as a rim around matrix Di + Pl symplectite; (3) in coronae around kyanite; and (4) in Prg + Pl symplectite around garnet. The composition of plagioclase is homogeneous within a single domain such as Di + Pl, but changes abruptly at the domain boundaries (Fig. 5). Plagioclase in coronae is anorthite in composition ($An_{89-97}Ab_{3-1}Or_{0-1}$) (Fig. 5a). The plagioclase rim around matrix Di + Pl symplectite has the composition $An_{35-38}Ab_{62-65}Or_{0-1}$; the vermicular plagioclase within the matrix symplectite of Di + Pl or Ed + Pl has a composition of $An_{30-33}Ab_{66-69}Or_{0-1}$ (Fig. 5a). There is no difference in An content associated with the presence or absence of the edenite in the matrix symplectite, however, the presence of edenite has a significant effect on the composition of plagioclase in the inclusion symplectite; plagioclase within a diopside matrix is $An_{36-42}Ab_{58-63}Or_{0-1}$ (Fig. 5b, symplectite) while that in contact with edenite is $An_{46-49}Ab_{51-53}Or_{0-1}$ (Fig. 5b, Ed + Pl). The plagioclase in a Prg + Pl symplectite around a garnet porphyroblast has a relatively homogeneous composition of $An_{73-85}Ab_{15-27}Or_{0-1}$ (Fig. 5c, Prg + Pl). The plagioclase in Ed + Pl symplectite in contact with the Prg + Pl symplectite around garnet has a composition of $An_{30-45}Ab_{55-70}Or_{0-1}$ (Fig. 5c, Ed + Pl symplectite).

Amphibole

Amphibole is present in the symplectites after omphacites and in the Prg + Pl symplectite around garnet. The symplectitic amphibole around garnet is pargasite with a constant composi-

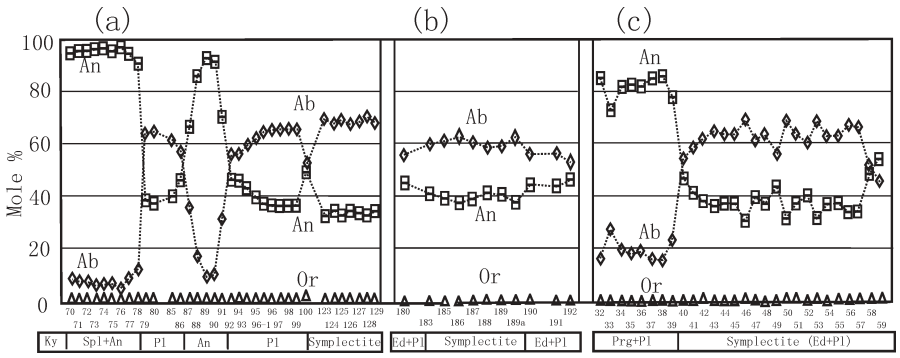

FIGURE 5. Compositional zoning profiles of plagioclase across: **(a)** both a corona around a kyanite grain and the adjacent symplectite after omphacite; **(b)** inclusion symplectite; and **(c)** both symplectite around a garnet and the adjacent matrix symplectite. For the analysis points, see Figures 3a, 3c, and 2d, respectively.

TABLE 2. Average values from microprobe analyses in the Rongcheng retrograde eclogite

Mineral*	Grt (R,6)	Grt (C,19)	Di (M,9)	Di (I, 11)	Omp (I)	Ttn	Prg (7)	Ed (M, 8)	Pl (Co, 7)	Pl (S, 8)	Pl (M, 6)	Pl (I, 6)	Pl (F, 6)	Spl	Grt	Prg	Pl
SiO_2	39.68	40.51	53.91	53.66	55.79	30.39	43.53	51.98	43.67	46.85	60.12	58.06	58.95	0.54	40.31	44.65	49.50
TiO_2	0.02	0.05	0.09	0.14	0.11	34.99	0.19	0.24	–	–	–	–	–	0.27	0.60	0.21	
$Al2O_3$	22.13	22.47	1.48	3.98	9.13	3.21	15.28	6.03	35.65	33.32	25.34	25.80	26.54	62.08	22.44	14.55	32.92
Cr_2O3	0.18	0.16	–	0.24	0.05	0.02	0.24	0.15	–	–	–	–	–	–	0.12	0.28	
FeO	18.17	14.87	4.33	3.47	1.64	0.50	9.40	7.59	–	–	–	–	–	24.85	14.76	8.23	
MnO	0.50	0.34	0.12	0.05	0.06	0.03	0.12	0.08	–	–	–	–	–	0.22	0.38	0.08	
MgO	10.96	13.56	15.45	14.59	11.75	0.00	13.80	17.97	–	–	–	–	–	10.62	12.92	14.75	
CaO	8.09	8.04	23.69	22.34	17.82	28.21	11.69	12.06	19.21	16.56	6.72	8.13	7.66	0.43	8.82	11.98	15.19
Na_2O	0.05	0.05	0.58	1.30	4.55	0.02	2.13	0.77	0.62	1.96	7.90	7.02	7.52	0.06	0.04	1.96	3.14
K_2O	0.00	–	0.00	0.01	–	–	0.34	0.08	0.01	0.03	0.05	0.04	0.05	0.02	0.00	0.02	0.02
Total	99.60	99.86	99.65	99.688	100.99	97.37	96.72	96.96	99.90	98.73	100.14	99.35	100.78	99.09	100.49	97.22	100.77
O(+OH)	12	12	6	6	6	5.002	24	24	8	8	8	8	8	4	12	24	8
Si	2.977	2.980	1.977	1.953	1.965	1.000	6.098	7.288	2.031	2.219	2.672	2.615	2.617	0.012	2.965	6.404	2.243
Al	1.956	1.947	0.064	0.171	0.378	0.125	2.522	0.994	1.952	1.817	1.326	1.369	1.386	1.960	1.946	2.460	1.759
Ti	0.001	0.003	0.002	0.004	0.003	0.866	0.020	0.025	–	–	–	–	–	0.001	0.033	0.023	
Cr	0.009	0.009	0.003	0.007	0.001	–	0.027	0.017	–	–	–	–	–	0.007	0.007	0.032	
Fe^{3+}†	0.079	0.046	0.015	0.001	–	–	1.102	0.554	–	–	–	–	–	0.009	0.056	0.237	
Fe^{2+}	1.062	0.869	0.118	0.101	0.048	0.012	0.000	0.323	–	–	–	–	–	0.569	0.852	0.750	
Mn	0.032	0.021	0.004	0.0017	0.002	–	0.014	0.007	–	–	–	–	–	0.005	0.024	0.010	
Mg	1.223	1.487	0.845	0.793	0.617	–	2.882	3.767	–	–	–	–	–	0.419	1.416	3.153	
Ca	0.651	0.633	0.931	0.873	0.672	0.995	1.755	1.812	0.946	0.822	0.320	0.392	0.364	0.013	0.659	1.841	0.738
Na	0.008	–	0.041	0.092	0.310	0.001	0.580	0.208	0.056	0.176	0.681	0.613	0.646	0.011	0.006	0.545	0.276
K	–	–	–	–	–	–	0.061	0.015	–	0.002	0.003	0.002	–	0.000	0.000	0.057	0.001
Total	8.000	7.993	3.999	4.000	4.000	3.000	15.061	15.015	4.985	5.035	5.002	4.991	5.013	3.005	8.000	15.510	5.016

Microprobe analyses for P–T calculations

End-member‡	Alm27.58	Alm28.55	WEF95.6	WEF90.6	WEF68.33	Ab5.5	Ab17.56	Ab67.83	Ab60.83	Ab63.77
	And4.53	And2.86	Jd3.44	Jd9.07	Jd31.67	An94.41	An82.25	An31.9	An38.97	An35.97
	Grs17.99	Grs17.20	Ae1.03	Ae0.37	Ae0.00	Or0.10	Or0.12	Or0.27	Or0.28	Or0.27
	Prp48.60	Prp50.09								

* Numbers in parentheses are the number of analyses used for the average. Other symbols in parentheses are: R = rim; C = core; M = matrix symplectite; I = inclusion; Co = corona; S = Prg + Pl symplectite; and F = the plagioclase film around symplectite after omphacite.
† Ferric iron is calculated after Droop (1987).
‡ Mineral abbreviations after Kretz (1983), other symbols: WEF, Wo + En + Fs; Ae, aegirine.

tion, whereas the amphibole in the symplectite after omphacite is edenite with variable compositions (Fig. 6). Both types of amphibole have constant CaO and Na_2O contents, with $Ca_B \geq 1.5$ and $^{VI}Al \geq Fe^{3+}$ (Ca_B, ^{VI}Al and Fe^{3+} calculated following the method of Leake et al. 1997).

MATERIAL TRANSFER

Method

Although the bulk composition of the coronae or symplectites and their real volume variations are not clear, we can quantify the material transfer by using the volumetric proportions of reaction products with the method developed by Gresens (1967), as shown for similar coronae by Godard and Mabit (1998). Godard and Mabit (1998) expressed the mass balance for formation of the corona or symplectite replacing a primary mineral (*P*) as:

$$1P + \mathbf{X} = \alpha A + \beta B + \gamma C + \ldots \quad (1)$$

where α, β, γ … are stoichiometric coefficients; *A*, *B*, *C*… are product minerals; and **X** is a vector (X_{Si}, X_{Al},..., X_{Na}) representing the material transfer between the system and its surroundings. If X_i is zero, the system is closed for the considered element *i*; otherwise, X_i represents the gain (positive value) or loss (negative value) of the element.

For a given element *i*, X_i can be expressed by the following equation:

$$X_i = F_v V_P (X_{vol}^{A} M_i^{A}/V_A + X_{vol}^{B} M_i^{B}/V_B + X_{vol}^{C} M_i^{C}/V_C + \ldots) - M_i^{P} \quad (2)$$

where F_v is the volumetric factor defined as $(\Delta V/V) + 1$ indicating variation in volume during the pseumorphism (Gresens 1967); V_A, V_B, V_C … and V_P are the molar volumes of the minerals that constitute the symplectite and the primary mineral, respectively; X_{vol}^{A}, X_{vol}^{B}, X_{vol}^{C}… represent the volumetric proportions of product minerals in the corona or symplectite; M_i is the quantity of element *i* in the considered mineral. In this study, three systems are defined to estimate their material transfers: kyanite and its coronae; garnet and its symplectite; and omphacite pseudomorphs. Seven elements (*i* = 1, 7 corresponding to Si, Al, Mg, Ca, Fe, Na, and O respectively) contained in omphacite, kyanite, garnet and their pseudomorphs are taken into consideration. The molar volume data are from Holland and Powell (1998). Microprobe analyses (Table 1) are used for M_i. The calculation process is the same as that of Godard and Mabit (1998), and results are listed in Table 2.

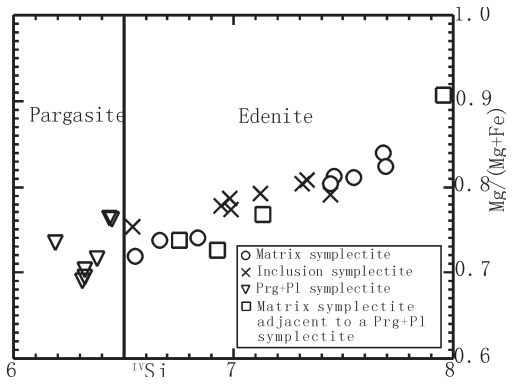

FIGURE 6. Si-Mg/(Mg + Fe^{2+}) projections of amphibole in the Rongcheng retrograde eclogite (after Leake et al. 1997). All amphiboles from symplectites after omphacite are located in the edenite area, while those in symplectites after garnet are at pargasite area.

Results

The kyanite + corona system. We tested the three primary eclogite-facies minerals (garnet, omphacite, and kyanite) and the whole-rock system; results for the breakdown of kyanite are shown in Table 1. The calculation also indicates that the X_i (in column 5)-X_i (in column 6) values listed in column 7 of Table 1 yield anorthite with the same composition as that in the corona around kyanite, demonstrating that the above calculation is reasonable.

The omphacite pseudomorph system. The composition of a primary omphacite can be restored based on the whole-rock composition, modal mineralogy, and the compositions of the other minerals in the rock, provided the material exchange has not occurred between the rock and its surroundings. However, our estimate demonstrates that the rock formed in an open system during decomposition. The restored omphacite cannot be used as a primary omphacite to estimate the material transfer that is related to its breakdown.

Fortunately, the kyanite porphyroblasts contain omphacite inclusions. Nakamura and Hirajima (2000) had demonstrated that there was no difference between the compositions of inclusion and matrix omphacite in less-symplectized Rongcheng eclogite. The matrix omphacite in the studied eclogite is retrograded, but inclusions in kyanite are unchanged. Here we take the omphacite inclusion (Table 2, Omp) in kyanite porphyroblasts as the primary omphacite. Results of the calculations are shown in column 3 of Table 1.

The garnet + symplectite system. The compositional zoning present in garnet discussed earlier (Figs. 3c and 3d) is common in eclogite (Nakamura and Hirajima 2000), and indicates that Fe-Mg exchange occurred between garnet and omphacite before their breakdown; this compositional zoning in the partially symplectized garnet grains has been destroyed during symplectite formation. The average microprobe analysis for garnet with symplectite [Table 2, Grt (rim)] was used to estimate mass balance during symplectization (see Table 1, column 4).

Whole-rock system. Omphacite (70 mol%), kyanite (12.5 mol%), garnet (11.5 mol%), rutile (3 mol%), and quartz (2 mol%) define the whole-rock system of the Rongcheng eclogite. Microscopic observations indicate that 100% of the matrix omphacite, about 80% of the kyanite, 10% of the garnet, and about 50% of the rutile have broken down (Table 1, row 1, percentages in parentheses). Based on the material transfer estimate (Table 1) and Equation 1, the breakdown of the eclogite minerals can be expressed by the equations listed in Table 3.

DISCUSSION

Element transport and mineral reactions

In this study, microtextures indicate that reactions occurred between kyanite and omphacite, or between garnet and omphacite, resulted in the formation of coronae around kyanite or garnet grains and symplectites after omphacite. Furthermore, estimation of material transfer demonstrates that the three major minerals and their pseudomorphs formed three open micro-systems. We now evaluate the extent to which there may have been mass transfer between those micro-systems by dissolution -precipitation reactions.

Dissolution and discontinuous precipitation relating to the growth of coronae around kyanite grains occurred along the boundary of the kyanite grain and progressed inward. Some Al in the kyanite was dissolved, and the remaining Si and Al were combined with Fe, Mg, and Ca to form spinel and anorthite. Similarly, during symplectite growth around garnet grains, dissolution and discontinuous precipitation began along the garnet boundary and progressed inward. Magnesium and Fe were partially dissolved, and the remaining elements were combined with extra Si, Al, Ca, Na, and OH to form the symplectite.

The symplectite after omphacite grains, with minor plagioclase as rods in the diopside host, very much resembles myrmekite (Figs. 3a, 3c). This texture suggests that there were many reaction sites within the primary omphacite. We assumed that the following discontinuous reactions have taken place within an omphacite grain, which have not only formed a symplectite (a pseudomorph after omphacite), but also provided Ca, Mg, and minor Fe to its surroundings:

$$Na_2O{\cdot}Al_2O_3{\cdot}4SiO_2 \text{ (Jd in Omp)} + CaO{\cdot}MgO{\cdot}2SiO_2 \text{ (Di in Omp)} \rightarrow 2NaAlSi_3O_8 \text{ (Ab)} + CaO + MgO \quad (3)$$

$$2(CaO{\cdot}Al_2O_3{\cdot}SiO_2) \text{ (Ca-Ts in Omp)} + CaO{\cdot}FeO{\cdot}2SiO_2 \text{ (Hd in Omp)} \rightarrow 2CaAl_2Si_2O_8 \text{ (An)} + CaO + FeO \quad (4)$$

Reaction 3 and 4 can be used to decipher the dissolution of Mg, Fe, and Ca from the omphacite. Precipitation is assumed to have occurred simultaneously. Extra Al, Si, and minor Na combined with part of the dissolved elements to form the plagioclase film around the symplectite.

The estimate of material transfer (see Table 1) indicates that Fe^{2+} from a decomposed omphacite is minor, suggesting Reaction 4 was not significant. Microprobe analysis reveals that the spinel in a corona around kyanite contains more Fe^{2+} than Mg (Mg/Fe $\approx$ 0.77), suggesting that some of the Fe in the spinel came from the breakdown of garnets. The Prg + Pl intergrowth replacing garnet produced extra Fe (Table 1).

TABLE 3. Equations showing the breakdowns of eclogite-facies minerals in the Rongcheng eclogite

Ky System	Inner Corona	$1Ky + 0.0955Mg + 0.1281Fe^{2+} + 0.2754Ca - 0.395Si - 0.9788Al - 1.788O \rightarrow 0.275An + 0.224Spl$*
	Outer Corona	$0.4514Si + 0.4346Al + 0.2128Ca + 0.0123Na + 1.778O \rightarrow 0.225An$
	Whole Corona	$1Ky + 0.0955Mg + 0.1279Fe + 0.4882Ca + 0.0564Si + 0.0123Na - 0.5442Al \rightarrow 0.500An + 0.224Spl$
Grt System		$1Grt + 0.3355Si + 0.3366Al + 0.4926Ca + 0.2737Na + 0.1802OH - 0.697\ Mg - 0.8605\ Fe^{2+} - 0.0794Fe^{3+} \rightarrow 0.1736Prg + 1.002Pl$
Omp System		$1Omp + 0.027Si + 0.226Al + 0.003\ Na - 0.263Mg - 0.141Ca - 0.002Fe \rightarrow 0.4206Drv + 0.4342Andesine$
Rt System		$1Rt + 1.1548Si + 0.1439Al + OH(or\ F) \rightarrow 1\ Ttn$

* The minus signs on the left side of each term indicate dissolution of the corresponding element, whereas the plus signs indicate precipitation.

In summary, there are three micro-metasomatic domains related to the breakdown of kyanite, garnet, and omphacite, and that element transport among them was widespread. Evidently, Al transfers from kyanite to garnet and omphacite; Mg from garnet and omphacite to kyanite; Ca from omphacite to garnet and kyanite, and Fe from garnet to kyanite.

Mass transfer also may have occurred between the eclogite and its host rocks. The estimate of material transfer demonstrates that the breakdown of all omphacite, garnet, and kyanite required extra Si (Table 2); this requirement can be met by primary quartz (formerly coesite) in the eclogite, which is no longer present due to extensive retrogression. The breakdown of the omphacite, garnet, and kyanite required Na and minor H_2O; host rocks could have provided these elements. The Al produced from the breakdown of kyanite was insufficient for the breakdown of garnet and omphacite, but the remainder could have come from the host rocks. The Mg and Ca produced by omphacite and garnet were not fully consumed by the formation of the coronae around kyanite, and would have been transferred to the host rocks where it was used in other reactions.

P-T estimates and implications

The above discussion suggests that the breakdown of the Rongcheng eclogite occurred under open-system conditions. Equilibrium was not reached at the whole-rock scale. However, in the micro-system scale, local equilibrium among adjacent minerals was reached (Thompson 1959) as revealed by mineral analyses. Such mineral parageneses can be used to estimate retrograde *P–T* conditions according to reactions among their end-members.

THERMOCALC (Holland and Powell 1998) was used to estimate *P* and *T* of Grt + Prg + Pl around a garnet porphyroblast. Microprobe analyses of the three minerals that are in direct contact were used as input data (Table 2, three right columns). Five independent reactions (Table 4) using end-member compositions of adjacent grains yielded $T = 655\pm70$ °C and $P = 1.3\pm0.2$ GPa. Such low temperatures could have preserved the compositional zoning in garnet (Ghent 1988; Ganguly et al. 1998). This new temperature estimate is much lower than the 700 to 800 °C proposed by Nakamura and Hirajima (2000), but this new pressure estimate is higher than their values of 0.7–1.2 GPa.

Textures in Rongcheng eclogite (Fig. 2) indicate that the eclogite was strongly deformed before retrogression resulting in a preferred orientation of elongate eclogite-facies minerals. This deformation created a path for hydrous fluids resulting in a very different retrograde assemblage from other Rongcheng eclogite samples. This heterogeneity suggests that temperature estimates within the UHPM Sulu terrane may be due to localized deformation and fluid activity.

TABLE 4. Calculated independent set of reactions using THERMOCALC software

(1) $2Prp + 4Grs + 3Ts + 12Qtz = 3Tr + 12An$
(2) $6Tr + 21Ab = 10Prp + 11Grs + 27Qtz + 6H_2O$
(3) $6Fac + 21An = 11Grs + 10Alm + 27Qtz + 6H_2O$
(4) $3Tr + 6Prg + 18An = 4Prp + 8Grs + 6Ts + 3Gln$
(5) $3Tr + 3Ts + 6Prg + 18Ab = 4Prp + 8Grs + 12Gln$

ACKNOWLEGMENTS

Chinese Natural Science Foundation (NSF, no. 40399141 to Chinese Continental Scientific Drilling (CCSD) Project and no. 40102018 to T.N. Yang) financially supported this study. This project was particially supported by U.S. NSF-EAR 0003355. We thank H. De Wall and A. Kontny for their generous help with microprobe analysis. Constructive reviews from R.F. Dymek, J.C. Schumacher, P. O'Brien, Simon Cuthbert, and Craig Manning are also gratefully acknowledged. Special thanks are given to J.G. Liou for his helpful suggestions.

REFERENCES CITED

Anovitz, L.M. (1991) Al zoning in pyroxene and plagioclase: window on late pro-grade to early retrograde *P-T* paths in granulite terranes. American Mineralogist, 76, 1328–1343.

Ashworth, J.R. and Chambers, A.D. (2000) Symplectic reaction in olivine and the controls of intergrowth spacing in symplectites. Journal of Petrology, 41, 285–304.

Austrheim, H. (1998) Influence of fluid and deformation on metamorphism of the deep crust and consequences for the geodynamics of collision zones. In B.R. Hacker and J.G. Liou, Eds., When continents collide: geodynamics and geochemistry of ultrahigh pressure rocks, p. 203–239. Kluwer Academic Publishers, Netherlands.

Carlson, W.D. and Johnson, C.D. (1991) Coronal reaction textures in garnet amphibolites of the Llano Uplift. American Mineralogist, 76, 756–772.

Cong, B.L. and Wang, Q.C. (1994) Review of research on ultrahigh-pressure metamorphic rocks in China. Chinese Science Bulletin (English edition), 39, 2068–2075.

Droop, G.T.R. (1987) A general equation for estimating Fe^{3+} concentrations in ferromagnesian silicates and oxides from microprobe analyses using stoichiometric criteria. Mineralogical Magazine, 51, 431–435.

Ganguly, J., Cheng, W.J. and Chakraborty, S. (1998) Cation diffusion in aluminosilicate garnet: experimental determination in pyrope-almandine couples. Contributions to Mineralogy and Petrology, 131, 171–180.

Ghent, E.D. (1988) A review of chemical zoning in eclogite garnets. In David C. Smith Ed., Eclogite and eclogite-facies rocks, p. 217–231. Elsevier, Amsterdam.

Godard, G. and Mabit, J. L. (1998) Peraluminous sapphirine formed during retrogression of a kyanite-bearing eclogite from Pays de Leon, Armorican Massif, France. Lithos, 43, 15–29

Gresens, R.L. (1967) Composition-volume relationships of metasomatism. Chemical Geology, 2, 45–65.

Holland, T.J.B. (1980) The reaction albite = jadeite + quartz determined experimentally in range 600-1200 °C. American Mineralogist, 65, 129–134.

Holland, T.J.B. and Powell, R. (1998) An internally consistent thermodynamic data set for phases of petrological interest. Journal of Metamorphic Geology, 16, 309–343.

Johnson, C.D. and Carlson, W.D. (1990) The origin of olivine-plagioclase coronae in metagabbros from the Adirondack Mountain, New York. Journal of Metamorphic Geology, 8, 697–717.

Kretz, R. (1983) Symbols for rock-forming minerals. American Mineralogist, 68, 277–279.

Leake, B.E., Wooley, A.R., Arps, C.E.S. and another ten authors (1997) Nomenclature of amphiboles: Report of the subcommittee on amphiboles of the International Association Commission on New Minerals and Mineral Names. Mineralogical Magazine, 61, 295–321.

Liati, A. and Seidel, E. (1996) Metamorphic evolution and geochemistry of kyanite eclogite in central Rhodope, Northern Greece. Contributions to Mineralogy and Petrology, 123, 293–307.

Liu, F.L, Xu, Z.Q. and Yang, J.S. (2001) Inclusions in the zircons within gneiss from

the pre-pilot bore hole CCSD-PP2, Subei, China, and the evidence for UHP metamorphism. Chinese Science Bulletin, 46, 241–244. (in Chinese)

Markl, G., Foster, C.T. and Bucher, K. (1998) Diffusion-controlled olivine corona textures in granitic rocks from Lofoten, Norway: calculation of Onsager diffusion coefficients, thermodynamic modeling and petrological implications. Journal of Metamorphic Geology, 16, 607–623.

Mørk, M.B.E. (1985) A gabbro to eclogite transition on Flemsøy, Sunnmøre, Western Norway. Chemical Geology, 50, 283–310.

Möller, C. (1998) Decompressed eclogites in the Sveconorwegian (-Grevillian) orogen of SW Sweden: petrology and tectonic implications. Journal of Metamorphic Geology, 16, 641–656.

Mysen, B. and Griffin, W. L. (1973) Pyroxene stoichiometry and the breakdown of omphacite. American Mineralogist, 58, 60–63.

Nakamura, D. and Hirajima, T. (2000) Granulite-facies overprinting of ultrahigh pressure metamorphic rocks, northeastern Su-Lu region, eastern China. Journal of Petrology, 41, 563–582.

Rubie, D.C. (1990) Role of kinetics in the formation and preservation of eclogites. In D.A. Carswell, Ed., Eclogite facies Rocks, p. 111–140. Blackie, Glasgow,

Thompson, J.B. (1959) Local equilibrium in metasomatic processes. In P.H. Abelson, Ed., Research in geochemistry, 427–457. Wiley, New York.

Wallis, S.R., Ishiwatari, A., Hirajima, T, Ye K., Guo, J., Nakamura, D., Kato, T., Zhai, M., Enami, M., Cong, B., and Bano, S. (1997) Occurrence and field relationships of ultrahigh pressure metagranitoid and coesite eclogite in the Sulu terrane, eastern China. Journal of the Geological Society. London, 154, 45–54.

Wang, Q.C., Ishiwatari, A., Zhao, Z., and Hirajima, T. (1993) Coesite-bearing granulite retrograded from eclogite in Weihai, eastern China. Europe Journal of Mineralogy, 5, 141–152.

Wang, Q.C., Zhai, M.G., and Cong, B.L. (1996) Regional geology, In C. Bolin, Ed., Ultrahigh pressure metamorphic rocks in the Dabie-Sulu region of China, 8–26. Science Press, Beijing, and Kluwer Academic Publishers, Boston.

Wang, X. and Liou, J.G. (1991) Regional ultrahigh-pressure coesite-bearing eclogite terrane in central China: evidence from country rocks, gneiss, marble and metapelite. Geology, 19, 933–936.

Wang, X., Zhang, R., and Liou, J.G. (1995) UHPM terrane in east central China. In R.G. Coleman and X. Wang, Eds., Ultrahigh pressure metamorphism, p. 353–390. Cambridge University Press, London.

Wikström, A. (1970) Electron microprobe studies of the alteration of omphacite in eclogites from the Nordfjord area, Norway. Norsk Geologisk Tidsskrift, 50, 135–155.

Xu, S.T., Okay, A.I., Ji, S., Sengor, A.M.C., Su, W., Liu, Y., and Jiang, L.L. (1992) Diamond from the Dabie Shan metamorphic rocks and its implication for tectonic setting. Science, 256, 78–82.

Yang, J.J., Godard, G., Kienast, J.R., Lu, Y., and Sun, J.X. (1993) Ultrahigh-pressure (60 kbar) magnesite-bearing garnet peridotite from northeastern Jiangsu, China. Journal of Geology, 101, 541–554.

Yang, J.J., Godard, G., and Smith, D.C. (1998) K-feldspar-bearing coesite pseudomorphs in an eclogite from Lanshantou (eastern China). European Journal of Mineralogy, 10, 969–985.

Ye, K., Yao, Y.P., Katayama, I., Cong, B.L., Wang, Q.C., and Maruyama, S. (2000a) Large areal extent of ultrahigh pressure metamorphism in the Sulu UHP terrane of eastern China: new implications from coesite and omphacite inclusions in zircon of granitic gneiss. Lithos, 52, 157–164.

Ye, K., Cong, B.L., and Ye, D.N. (2000b) The possible subduction of continental material to depths greater than 200km. Nature, 407, 734–736.

Yin, A. and Nie, S.Y. (1993) An indentation model for the North and South China collision and the development of the Tanlu and Honam fault systems, eastern Asia. Tectonics, 12, 801–813.

Zhang, R. and Liou, J.G. (1997) Partial transformation of gabbro to coesite-bearing eclogite from Yangkou, the Sulu terrane, eastern China. Journal of Metamorphic Geology, 15, 183–202.

Zhang, R, Hirajima, T., Banno, S., Cong, B., and Liou, J.G. (1995) Petrology of ultrahigh pressure rocks from the southern Su-Lu region, eastern China. Journal of Metamorphic Geology, 13, 659–675.

MANUSCRIPT RECEIVED MAY 16, 2003
MANUSCRIPT ACCEPTED APRIL 25, 2004
MANUSCRIPT HANDLED BY ROBERT F. DYMEK